View metadata, citation and similar papers at core.ac.uk

brought to you by CORE

provided by VBN

Aalborg Universitet

AALBORG UNIVERSITY
DENMARK

Inducverters: PLL-Less Converters with Auto-Synchronization and Emulated Inertia Capability

Ashabani, Mahdi; Freijedo Fernandez, Francisco Daniel; Golestan, Saeed; Guerrero, Josep M.

Published in:
I E E E Transactions on Smart Grid

DOI (link to publication from Publisher):
10.1109/TSG.2015.2468600

Publication date:
2016

Link to publication from Aalborg University

Citation for published version (APA):
Ashabani, M., Freijedo Fernandez, F. D., Golestan, S., & Guerrero, J. M. (2016). Inducverters: PLL-Less Converters with Auto-Synchronization and Emulated Inertia Capability. I E E E Transactions on Smart Grid, 7(3), 1660 - 1674. DOI: 10.1109/TSG.2015.2468600

General rights
Copyright and moral rights for the publications made accessible in the public portal are retained by the authors and/or other copyright owners and it is a condition of accessing publications that users recognise and abide by the legal requirements associated with these rights.

? Users may download and print one copy of any publication from the public portal for the purpose of private study or research.
? You may not further distribute the material or use it for any profit-making activity or commercial gain
? You may freely distribute the URL identifying the publication in the public portal ?

Take down policy
If you believe that this document breaches copyright please contact us at vbn@aub.aau.dk providing details, and we will remove access to the work immediately and investigate your claim.

Downloaded from vbn.aau.dk on: April 29, 2017

Inducverters: PLL-Less Converters with Auto-Synchronization and Emulated Inertia Capability

Mahdi Ashabani, Francisco Freijedo, *Member, IEEE*, Saeed Golestan, *Senior Member, IEEE*, and Josep M. Guerrero, *Fellow, IEEE*

Abstract–In this paper, the idea of operation of grid connected voltage source converters (VSCs) by similar characteristics of induction machines under new concept of *inducverter* is proposed and developed. The proposed controller eliminates the need for an extra synchronization unit and phase-locked-loop (PLL). Therefore, it offers a simpler and more reliable control strategy with improved performance, as it provides real auto-start and auto-synchronization with a grid without the need for grid voltage information. A current damping/synchronization unit enables grid auto-synchronization by using local current information and can track grid frequency, angle and voltage amplitude variations while feeding constant amount of power which is of high interest in frequency varying grids and also in the case of grid voltage angle jump. Another advantage of the inducverter is that it introduces virtual inertia to the grid to regulate frequency which enhances frequency dynamics of smart grids. Beside the current synchronization unit, the proposed strategy has a single-loop controller core with control over both power and current which is implemented in a hybrid *dq* and *abc* frame using a virtual adaptive lead or lag impedance. The controller also offers stable and high-performance synchronization and operation under unbalanced and/or distorted grid conditions. The work beside synchronous current converters give a bird's eye view to research in the new area of PLL-less and virtual inertia-based operation of VSCs and fulfill a unified set of controllers for the smart grid integration. Simulation, hardware-in-loop (HIL) and experimental results are presented to validate effectiveness of the controller.

***Index Terms*— Emulated inertia, grid synchronization, induction machine, phase-locked-loop, smart grid, voltage source converter.**

I. Introduction

The paradigm of smart grid is rapidly changing the operation and control of the conventional power systems mainly because of extensive use of power electronic devices and communication infrastructure. Fast development of renewable energy resources and electronically interfaced (EI) generations and loads such as wind turbines, solar cells and adjustable speed drives are the basic reasons that make the control of VSCs the core of concerns of smart grids operation as it is expected that more than 60% of generation and load units will be EI ones in the early future [1]-[2]. However, converter dominated smart grids are facing severe stability and control challenges such as instabilities due to frequent transitions between islanding and grid connected modes which necessitates smooth grid synchronization, restoration, and "only-plug" capability and also overall low inertia as a direct result of the elimination of the rotating mass in EI units which drastically degrades system stability and frequency regulation. Furthermore, with increasing share of EI loads and renewable energy resources, serious concerns about how to handle and operate VSCs in an environment with numerous conventional electrical machines such as line start machines, doubly fed induction generators and synchronous generators (SGs) have raised. Some discussions about the effects of high penetration level of VSCs into the grid can be found in [3-8]. Moreover, rather unpredictable behavior of conventional control strategies like the vector control due to their interactions with the conventional electrical machines [1], [9-14] has attracted considerable attention to the development of a new class of controllers in the context of smart grid integration.

To overcome these difficulties, it is possible to create a complicated and costly control and communication infrastructure to optimally coordinate and control EI units and conventional electrical machines-based generation units which necessitates creating a basically new control and monitoring framework. The alternative is to design a unified grid-friendly control strategy for EI and electrical machine-based units such that grid senses them the same and consequently, the operation, control and analysis of the future complex smart grids are simplified to the conventional power systems. Toward this, some new and advanced controllers have been recently proposed to make VSCs behave like SGs [9-24] or emulate the characteristics of VSCs in SGs [25]. The most comprehensive and unified ones are presented under umbrella of synchronous converter [12], [23-24] and synchronous-VSC [1] which are applicable to both islanded and grid-connected grids with grid self-tracking ability after initial synchronization. The *virtual synchronous generator* (VSG) [15-18] and *virtual synchronous machine* (VISMA) [19] are some other examples of emulating SGs in VSCs. Since these controllers act like an SG, they introduce some inertia for the frequency regulation known as virtual inertia. Actually, any source of energy connected to the dc-link of VSC can provide some virtual inertia. The question is that how to design suitable control mechanism to properly regulate system. It is shown in [1], [12], [14] that the conventional controllers fall short for this purpose. Synchronous converter, bidirectional synchronous-VSC and VSGs realize the inertial response similar to SGs. Although the virtual synchronous machines and virtual inertia can significantly improve the system stability in smart grids with consistent reduction in the overall system inertia, these types of controllers inherent the drawbacks of SGs such as hunting around the rated frequency and slower response.

Another basic requirement of VSCs operation in smart grids is their successful synchronization and connection with a grid with unknown frequency, angle and voltage amplitude at the moment of connection and keeping the synchronization even in the case of sudden variations of these parameters [9], [10], [12], [22], [26]. VSCs not only should synchronize themselves with the grid, but also it is essential that they inject constant amount of power to the grid regardless of variations of voltage frequency, angle and amplitude. To connect a VSC to a grid, it has been widely adopted in industry to use a synchronization unit, typically using a PLL, to estimate the grid's parameters and align VSC's voltage vector with the grid's one to guarantee smooth connection and avoid large transients due to out-of-phase closing [22], [23], [27]. Any large delay in the PLL and the synchronization process may cause instability [28]. Also, the instabilities due to low-frequency oscillations are well discussed in the literature [29]. Several works have been reported in recent years to improve synchronization speed and accuracy [27-32]. Therefore, the synchronization unit has a considerable effect on the performance

of VSC and its poor performance (e.g., due to improper tuning of its control parameters) may adversely affect the VSC dynamical behavior and even jeopardize the converter stability [10], [28]-[29]. This issue becomes more critical under the weak grid condition, islanded condition, and large penetration of DG units into the grid [29]. Therefore, the elimination of the need for a synchronization unit can be an interesting option in such scenarios.

To the authors' best knowledge, the idea of auto-synchronization and control of converters without using a dedicated synchronization unit, was firstly proposed in [33] and then continued in [22] and [23]. Although these techniques can achieve "only-plug" performance and self-synchronization, they are nonlinear controllers with complicated design and parameter adjustment. Reference [10] also aims at realizing self-synchronization ability in a VSC by adding a virtual current loop but it still requires the inception time and the grid voltage information to activate the virtual current loop.

This paper presents a new generation of controllers for VSCs with virtual inertia and PLL-less grid soft-synchronization capability and with dynamics similar to induction machines. This controller is a continuation of synchronous converters and synchronous-VSC to establish a unified and universal platform for the integration of VSCs in smart grids with improved stability and performance. The inducverter offers many advantages some of them listed as follows:

- It has real and true PLL-less operation and grid synchronization ability without the need for grid information. In fact, the controller, PLL and synchronization unit are integrated into one compact structure. The controller also can track grid voltage amplitude and frequency variations. The inducverter is advantageous to the basic synchronous converter [12], [22-23] and synchronous-VSC [1] since they cannot guarantee grid smooth synchronization without a supplementary nonlinear controller.
- The controller feeds constant amount of real and reactive powers to the grid regardless of variations of grid parameters. This is a major advantage as compared to the VSG [15-18], synchronous converter [12], [22-23] and synchronverter [10] where any deviation in the grid frequency results in a permanent offset in the output real and reactive powers.
- The integrated power damping unit also participates in the power system frequency regulation and stabilization by introducing virtual inertia. Actually, the controller resembles the characteristics of an induction machine.
- The controller is a single-loop one with both power and current regulation. It is implemented in a hybrid *abc* and *dq* frame where *dq*-axis current references are obtained according to the real and reactive power errors and these *dq*-axis current references are translated to *abc* voltage references by an adaptive virtual impedance in the *abc* frame.

In summary, the main contribution of the paper is introducing a new concept: PLL-less grid auto-synchronization without the grid information which is inspired by induction machine working principles as it has the same synchronization capabilities. To the best of the authors' knowledge, this idea has not been presented before and we believe it can open a broad view to this new research area. In addition, the controller inherently introduces some virtual inertia to the grid to improve frequency dynamics.

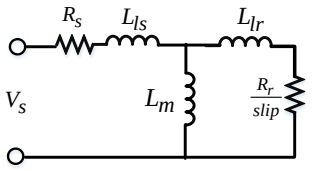

Fig. 1. Equivalent circuit of an induction machine.

Another contribution of the paper is using a hybrid single-loop control implemented in both *dq* and *abc* reference frames with both power and current control and regulation capability. PI controllers are used to generate *dq*-axis current references according to power references while lead-lag compensators are used to transform current references into three-phase voltage commands in the *abc* reference frame. The controller also offers superior high-performance grid synchronization under unbalanced and/or distorted grid conditions.

II. Induction Machine Working Principles

Invented more than one hundred years ago, induction machines modeling, analysis and control have reached high maturity. An induction machine is composed of two parts: a stator with symmetrical three-phase windings and a rotor which can be either squirrel cage or wound one. Given a three-phase voltage, the stator windings generate a rotating magnetic field. As the rotor of an induction motor is short-circuited by an end ring and cut the stator rotating magnetic field, some voltage is induced in the rotor causing some electric current flows in the rotor. Because of interaction between the stator and rotor magnetic fields some torque is generated in the machine at any rotor speed except at the synchronous speed. The induction motor cannot run at the synchronous speed because at the synchronous speed no voltage is induced in the rotor, the induction motor cannot develop torque. *Slip* in an induction machine is defined as

$$slip = \frac{\omega_s - \omega_r}{\omega_s} = \frac{\omega_{slip}}{\omega_s} \tag{1}$$

where ω_s , ω_r and ω_{slip} are the synchronous, slip and rotor frequency, respectively. Using space vector notation, the stator and rotor voltage equations for a short-circuited rotor induction machine are given by [34]-[35]

$$V_s = (R_s I_s + L_s p) I_s + L_m p I_r \tag{2}$$

$$0 = (R_r I_r + L_r (p - j\omega_r)) I_r + L_m (p - j\omega_r) I_s \tag{3}$$

where p denotes the derivation, and r and s stand for rotor and stator, $L_s = L_{ls} + L_m$ and $L_r = L_{lr} + L_m$ where L_{lr} , L_{ls} and L_m are rotor leakage, stator leakage and magnetizing inductances, respectively. In frequency domain, (2-3) are represented by

$$V_s = (R_s + sL_s) I_s + sL_m I_r \tag{4}$$

$$0 = \left(\frac{R_r}{slip} + sL_r \right) I_r + sL_m I_s . \tag{5}$$

According to these equations, the conventional steady state circuit of an induction machine is modeled as shown in Fig. 1. Therefore, the equivalent impedance of an induction machine relating its input current and terminal voltage is expressed by

$$Z_v = \frac{V_S}{I_S} = \frac{slip[(L_m + L_{lr})R_s + L_{ls}R_r + L_m R_r]s + R_s R_r}{[(L_{lr} + L_m)slip]s + R_r} + \tag{6}$$

$$+ \frac{slip[L_m L_{lr} + L_{ls}(L_m + L_{lr})]s^2}{[(L_{lr} + L_m)slip]s + R_r}$$

which describes the impedance characteristics of an induction machine and relates current and voltage. In other words, given a specific voltage waveform current waveforms can be obtained using this equation. Air gap power is calculated by

$$P_{ag} = 3|I_r|^2 \frac{R_r}{slip} \tag{7}$$

and output converted mechanical power (P_{mech}) and torque (T_e) are estimated by [34]

$$P_{mech} = (1-slip)P_{ag} = 3(1-slip)|I_r|^2 R_r / slip. \tag{8}$$

$$T_e \approx \frac{1}{\omega_s^2} \frac{V_s^2 \frac{R_r}{slip}}{\left(L_{ls}+L_{lr}\right)^2 + \left(\frac{R_r}{slip}\right)^2}. \tag{9}$$

Fig. 2 shows the power waveforms of an induction machine as a function of rotor speed and at different synchronous speed. As it is seen, when a machine, with arbitrarily initial rotor speed near to the synchronous speed (point A in Fig. 2) and constant load power on its shaft, is connected to a grid with frequency ω_{s0} , it generates some torque/power which enables it to start. Thus, an induction has self-start capability regardless of the grid frequency and voltage amplitude and after some time the rotor speed converges to an equilibrium point (point B), which is different from the synchronous or equivalently grid frequency, and provides the required output load power. Rotor speed depends on many factors like rotor resistance and inductance and output power. Another important factor in induction machine operation and also its self-start capability is its overall variable and adaptive equivalent impedance which provides a variable output power, almost proportional to the rotor slip, and enables it to adapt itself to load power and grid frequency variations. However, during the start-up process the output torque and currents may increase to several times of their nominal values. To overcome this difficulty, a soft-start process is usually adopted in which the terminal voltages of the machine are properly controlled to limit output power and currents.

Induction machines also offer another major advantage as their rotor stores some kinetic energy which can damp power and frequency oscillations by injecting or absorbing power during contingencies and participate in frequency control and regulation. For example, if the load power increases from P_1 to P_2 the rotor speed temporarily decreases to feed some short term energy to the load and damp load disturbance. After the power disturbance is damped, again rotor speed increases and recovers its new equilibrium point (point C). Moreover, an induction machine can easily switch from motoring mode to generative mode with slight change in the rotor speed. Simply speaking, when a machine working in motoring mode with a slight change in the rotor speed, it can increase to larger values of the synchronous speed and the machine can operate as a generator. Now suppose that the grid frequency reduces to ω_{s1} as shown in Fig. 2. The corresponding power/torque waveform for this grid frequency is shifted to the left. In this case, the rotor speed also converges to a new and unknown equilibrium point (point D). There is no need to know the grid frequency and also the rotor frequency since they are varied and adjusted simultaneously. It is worth taking into account that the induction machine can generate a constant output power or torque independent of variations of grid voltage

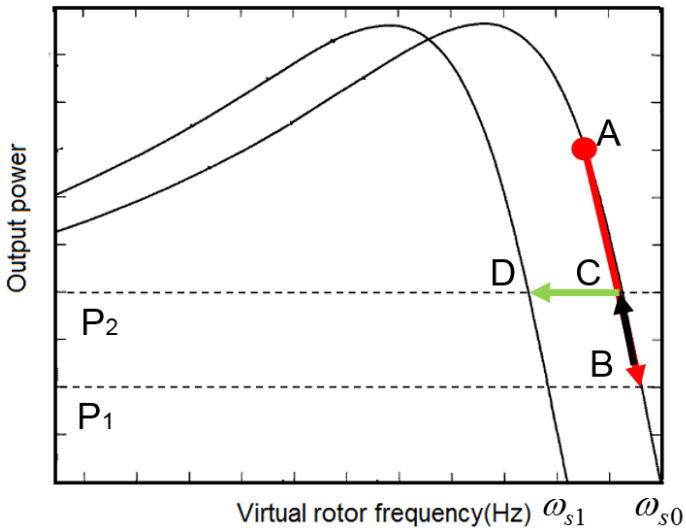

Fig. 2. Power/torque curve of an induction machine as a function of rotor frequency and at different synchronous frequencies.

frequency, angle and amplitude. Synchronous generators can also track grid voltage frequency and amplitude variations and synchronize themselves with the grid; however, any deviation in the grid frequency and voltage amplitude causes a permanent offset in output generated power which may saturate or overload the machine. This necessitates a mechanism to detect the grid frequency and correct the power and frequency set points to keep the output power constant. This needs a PLL which is in contradiction to the self-synchronization ability of synchronous generators.

III. INDUCVERTER

As discussed earlier, induction machines offer numerous advantages in terms of dynamic, operation and performance such as automatic grid soft-start and soft-synchronization, adaptive impedance behaviour, and power and frequency regulation due to the rotor inertia. In this paper, a new control strategy is developed called *inducverter* which emulates the dynamical behaviour of induction machines. The basic idea is simple and straightforward: if an induction machine has self- and soft-start capability and can automatically synchronize itself with a grid and track its variations without any information from the grid, a controller with the same dynamic features and characteristics can also realize these objectives. The inducverter also inherently enjoys the benefit of virtual inertia to enhance frequency and power regulation and grid senses the dc-link as a virtual rotor. Also, the concepts of adaptive virtual impedance and hybrid *dq/abc* frame control are introduced in this paper. The hybrid *dq/abc* control means that the controller is a single loop one which is implemented in both *dq* and *abc* frames. In fact, a vector controller generates the references of d- and q-axis currents as functions of the real and reactive power errors and virtual adaptive lead/lag compensators in polar *abc* coordinate adjust the three-phase voltages according to d- and q-axis reference currents. The overall controller consists of two main parts, namely the current/power damping and synchronization unit which generates the reference frequency and aims at grid soft and auto-synchronization and the second part is the core controller which adjusts three-phase voltage references such that the preset real and reactive powers are generated.

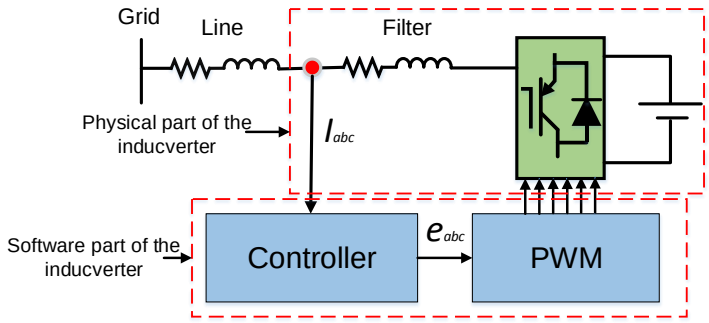

Fig. 3. Implementation and different parts of an inducverter.

A. *Current damping and synchronization unit*

In the conventional control strategies such as the vector control and direct power control a PLL is necessary to obtain the grid frequency and angle. Actually, the PLL plays two roles: firstly for the initial synchronization with the grid it is employed in a synchronization unit and when the voltage vectors of the VSC and the grid are aligned the breaker between them is closed. Any failure in this process results in out-of-phase closing and may cause instability and damage to VSC. Secondly, after initial grid synchronization, the PLL is responsible for estimation of grid voltage frequency and angle for the *abc* to *dq* frame transformation.

In this paper, an augmented controller and PLL strategy is developed in which a current damping/synchronization unit replaces both the synchronization unit and the PLL as it provides self- and soft-start and virtual inertia without the need for grid information. The inducverter has two main parts: an electrical part which is a real converter and the related RL or LCL filter shown in Fig. 3 and the second part is the control part which by proper voltage control enables the converter to behave similar to an induction machine. The control part generates PWM signals applied to the real converter. To obtain the model of the current damping unit, the equivalent model of an induction machine model in *dq* frame for a VSC mimicking its behaviour is given as follows:

$$V_{ds} = p\lambda_{ds} - \omega_s\lambda_{qs} + R_s I_{ds} \tag{10}$$

$$V_{qs} = p\lambda_{qs} + \omega_s\lambda_{ds} + R_s I_{qs} \tag{11}$$

$$V_{dr} = 0 = p\lambda_{dr} - \omega_{slip}\lambda_{qr} + R_r I_{dr} \tag{12}$$

$$V_{qr} = 0 = p\lambda_{qr} + \omega_{slip}\lambda_{dr} + R_r I_{qr} \tag{13}$$

where V_{ds} , V_{qs}, λ_{ds} and λ_{qs} are *dq*-axis voltages and stator flux linkages, respectively. Equations (12-13) represent the electrical model of a short-circuited rotor. The speed of rotation of the synchronous frame is ω_s which is a varying with time parameter. The governing equations for the rotor and stator flux linkages are

$$\begin{bmatrix}\lambda_{ds}\\ \lambda_{dr}\end{bmatrix} = \begin{bmatrix}L_s & L_m\\ L_m & L_r\end{bmatrix}\begin{bmatrix}I_{ds}\\ I_{dr}\end{bmatrix} \tag{14}$$

$$\begin{bmatrix}\lambda_{qs}\\ \lambda_{qr}\end{bmatrix} = \begin{bmatrix}L_s & L_m\\ L_m & L_r\end{bmatrix}\begin{bmatrix}I_{qs}\\ I_{qr}\end{bmatrix} \tag{15}$$

The virtual torque equation in this case is expressed by [35]

$$T = \frac{3}{2}(\lambda_{ds}I_{qs} - \lambda_{qs}I_{ds}) \tag{16}$$

The problem related with this modeling is that the synchronous speed (ω_s) should be known whereas the grid frequency in the modeling is considered as a variable and is unknown. Toward this, the grid frequency should be estimated as a function of other parameters and eliminated from the equations. As shown below, in steady state operation the proposed controller is able to synchronize the flux with d-axis. Then, in order to ease the dynamics analysis this situation is assumed: $\lambda_{dr} = K$ and $\lambda_{qr} = 0$. It should be noted that we decide the direction of the dq-frame, so in this case it is assumed the d-axis is aligned with the virtual rotor flux simplifying the torque equation. This is known as field-oriented control of induction machines which is very well-known in the literature [34], [35]. The same idea has been extensively used for the conventional voltage-based PLLs where the voltage angle is obtained such that voltage vector is aligned with the d-axis [36], [37]. In this case, with some math using equations (10-15) the virtual torque equation of (16) is simplified to

$$T_e = \frac{3}{2}\frac{L_m}{L_r}KI_{qs} \tag{17}$$

This indicates that the virtual torque and equivalently the real power are proportional to the q-axis current. Also, with assumption of $\lambda_{qr} = 0$, equations (12-13) are simplified to

$$R_r I_{dr} + p\lambda_{dr} = 0 \tag{18}$$

$$R_r I_{qr} + \omega_{slip}\lambda_{dr} = 0 \tag{19}$$

which yields

$$I_{qr} = -(\frac{L_m}{L_r})I_{qs} \tag{20}$$

$$I_{dr} = \left(\lambda_{dr} - L_m I_{ds}\right)/L_{lr} \tag{21}$$

Substituting these equations into (12-13), the following equations are obtained

$$\omega_{slip} = \left(L_m/\tau_r\right)\left(I_{qs}/\lambda_{dr}\right) \tag{22}$$

$$\tau_r\frac{d\lambda_{dr}}{dt} + \lambda_{dr} = L_m I_{ds} \tag{23}$$

where $\tau_r = L_{lr}/R_r$. So far the dynamics of the slip frequency is obtained. This frequency is unknown and can adapt itself to the output power, grid frequency and connecting line impedance variations. To obtain the dynamic of the output frequency and angle similar to a PLL, the mechanical dynamic of the virtual rotor is expressed by

$$\frac{d\omega_r}{dt} = \frac{1}{J}\left(T_e - T_L - D\omega_r\right) \tag{24}$$

where *J* is the momentum inertia of the virtual rotor and *D* is the virtual friction and damping and the generated output torque is given by (16). So in the frequency domain it has a first order low-pass filter characteristic and yields

$$\omega_r = \frac{1}{Js + D}\left(T_e - T_L\right) \tag{25}$$

The friction factor *D* also plays the role of power/torque drooping. Equations (24) and (25) overall describe the frequency

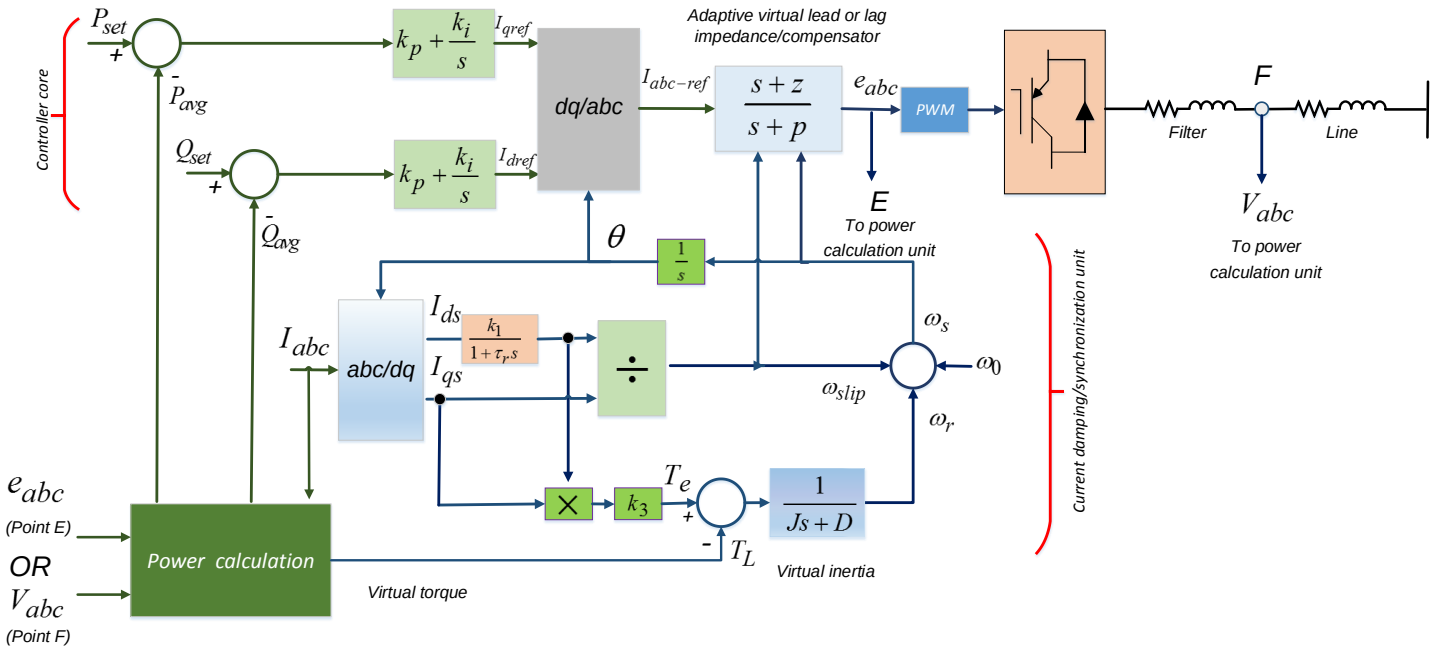

Fig. 4. Schematic view of the proposed induction power controller.

dynamics of the converter while (24) is the dominant term and the slip frequency of (22) adds an adaptive term which adjusts itself to grid voltage and also output power variations. Finally, the angle reference is calculated by

$$\theta = \int \left(\omega_r + \omega_{slip} + \omega_0\right) dt \tag{26}$$

where ω_0 is the rotor initial frequency. In fact, it is similar to connect an induction machine rotating at initial rotor speed of ω_0 to a grid. If ω_0 is selected some value near to the synchronous frequency, it can reduce frequency deviations and transients subsequent to the grid connection. The power damping unit is a closed loop unit where the output angle is fed back to the *abc/dq* transformation block and d- and q-axis currents are used to for the frequency calculation. The virtual rotor term J introduces some inertia to the system and regulate frequency. Actually, in an inducverter the d- and q-axis currents are calculated in the *abc* to *dq* block such that the grid senses the dc link as a virtual rotor which can feed or absorb short term energy to improve frequency stability. The size of virtual rotor inertia (J) can be calculated for small values of slip by equalizing the stored energy in the dc-link capacitor (C) and virtual rotor of the inducverter:

$$\frac{1}{2} J \omega_s^2 \approx \frac{1}{2} C V_{DC}^2 \tag{27}$$

Nevertheless, this equation does not take into account that there is a lower limit of the DC link voltage that allows the converter to operate correctly, while the converters are usually designed to optimize the DC Link voltage. To overcome this difficulty, the energy transferred through the dc-link capacitor within time interval of ΔT is set equal to the energy transferred by the virtual rotor inertia (J). The same approach was also adopted in [1], [13]. The describing power equation of the dc-link capacitor is expressed by

$$C V_{DC} \frac{dV_{DC}}{dt} = P_{in} - P_{out} \tag{28}$$

Assuming the grid frequency variations are small, which is normally the case, the power transfer equation of the virtual rotor can be obtained by using the same swing equation given in [41]:

$$M_m \frac{d\omega_r}{dt} = P_{in} - P_{out} \tag{29}$$

where $M_m = J\omega_s$.

Integrating both (28) and (29) within a time interval and equating them results in:

$$\int_{\omega_s}^{\omega} M_m d\omega_r = \int_{V_{DC0}}^{V_{DC}} C dV_{DC} \tag{30}$$

$$M_m(\omega - \omega_s) = \frac{1}{2} C (V_{DC}^2 - V_{DC0}^2) \tag{31}$$

$$M_m \Delta\omega = \frac{1}{2} C V_{DC0}^2 [(1 + \frac{\Delta V_{DC}}{V_{DC0}}) - 1] \tag{32}$$

$$J \approx \frac{C(V_{DC0}^2 / \omega_s^2)}{2} \frac{[(1 + \Delta V_{DC} / V_{DC0})^2 - 1]}{(\Delta\omega / \omega_s)} \tag{33}$$

In the above equations V_{DC0} is the initial DC link voltage. The time-constant of the frequency loop is expressed by

$$\tau_f = \frac{J}{D} \tag{34}$$

Larger values of J result in a better frequency regulation, but at the cost of a slower response. However, the damping factor D can be increased to present larger bandwidth and faster response. Since parameters are virtual, designer can select values for these parameters of the emulated inertia which are not practical for real machines. Similarly, the virtual electrical parameters such as τ_r

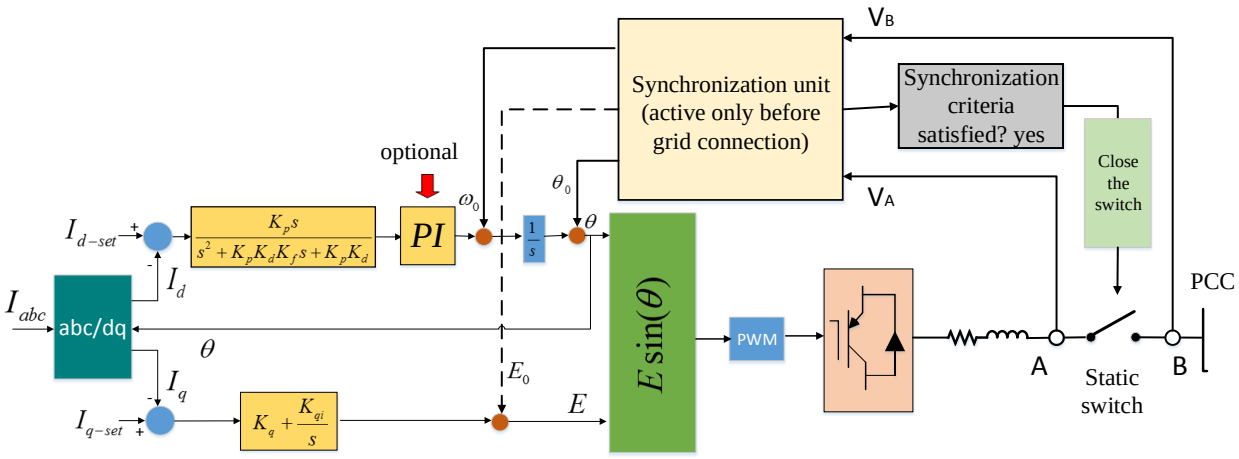

Fig. 5. Conventional synchronization process, applied to a synchronous current converter.

can take values which are not available for the real induction machines with the same power rating. However, the most straightforward approach is to adopt the parameters of the equivalent induction machine. Fig. 4 shows the implementation of the proposed inducverter. For the calculation of real and reactive powers and also virtual torque it is possible to use either voltage commands (e_{abc}) or filter voltage (point F in Fig. 4) by using voltage sensors. In the first case, no voltage sensor is required and the controller regulates filter power whereas in the second case voltage sensors are required and the injected powers to the line (after the filter) are controlled.

B. Controller core and adaptive virtual impedance

The main duty of the power damping unit is to properly estimate frequency and angle similar to a PLL using local information and realize self-synchronization. The core controller shown in Fig. 4 aims at generating preset values of the real and reactive powers using the angle reference given by the current damping/self-synchronization unit. According to equation (17), the virtual torque and real powers are controllable through the q-axis current. The core controller consists of two individual channels; the first channel controls and regulates real power by a simple proportional-integrator (PI) controller. In the same way, the second channel forces the error between the output reactive power and its reference to zero.

One interesting point of the proposed controller is that it is implemented in both *dq* and *abc* frame, i.e. it is a hybrid *abc/dq* frame control. The PI controllers tune the current references; however, three-phase voltage references are required to be applied to the converter. It is possible to use an inner voltage loop similar to the conventional vector control strategies in which d- and q-axis currents are fed back to the voltage loop and finally the d- and q-axis voltage references are obtained and applied to the VSC. Nevertheless, one more inner loop is necessary which in turn reduces overall bandwidth of the system and response speed as well. As an alternative, it is also possible to obtain the three-phase current references and calculate voltage references using virtual impedance. Since it is supposed that the controller presents the dynamic characteristics of an induction machine, the transfer function of the virtual impedance can be adopted from an equivalent induction machine in *abc* frame. The background philosophy is what the terminal voltages of an induction machine would be if a given current waveform is applied to it? Referring to equation (6) it is w**o**rth mentioning that since $L_m, L_{lr} << R_r, R_s$, the coefficient of s^2 is much smaller of other terms in the nominator and as an approximation it can be omitted. Thus, the virtual impedance transfer function Z_v is approximated as

$$Z_v \approx \frac{slip[(L_m + L_{lr})R_s + L_{ls}R_r + L_m R_r]s + R_s R_r}{[(L_{lr} + L_m)slip]s + R_r} \tag{35}$$

$$= \frac{s+z}{s+p}$$

$$z = \frac{R_s R_r}{slip[(L_m + L_{lr})R_s + L_{ls}R_r + L_m R_r]},\ p = \frac{R_r}{(L_{lr} + L_m)slip}$$

This represents an adaptive lead or lag compensator. Whether it is important to enhance the transient response or steady state error either lead or lag compensator can be selected. However, the locations of the zero and the pole for a given slip can be easily determined using the parameters of an induction machine with the same rated power.

IV. Conventional Grid Synchronization Method

VSCs in microgrid applications are connected to the main utility grid through a static switch at the point of common coupling (PCC) which is commonly remote from the VSCs. Fig. 5 shows the conventional synchronization process applied to a synchronous current converter [12]. The same process is also adopted for the connection of the conventional vector-control-based strategies. For smooth connection, the synchronization unit by proper voltage adjustment of the VSC makes the voltages difference of both sides of the static switch minimum. To this end, the voltages of points A and B are measured using voltage sensors and their frequency, angle and amplitude are extracted in synchro-phasor units, typically by a PLL [39]. This information is then fed back to the synchronization unit using a communication link, and the synchronization unit adjust the initial frequency

TABLE I. CRITERIA FOR STANDARD GRID SYNCHRONIZATION PROCESS [38]

Average rating of VSC	Frequency difference ($\Delta f, Hz$)	Voltage magnitude difference ($\Delta V, \%$)	Phase-angle difference ($\Delta\theta, \circ$)
0-500 kVA	0.3	10	20
>500-1500 kVA	0.2	5	15
>1500-10000 kVA	0.1	3	10

(ω_0), angle (θ_0) and amplitude (E_0) of voltage of VSC such that the difference of these variables at points A and B are kept within the acceptable limits for several cycles according to IEEE Std. 1547 [38] given in Table I. Consequently, in the conventional method, a PLL and related voltage sensors at each side of the static switch, and a communication link are needed. Moreover, a synchronization algorithm should be adopted to check synchronization criteria whereas any failure in accurate estimation of the grid voltage variables or slow synchronization process may result in unsuccessful grid synchronization.

Contrary to the conventional method, the inducverter does not require voltage sensors, synchronization unit, and communication links for normal operation and connection to the grid. These features make the structure of inducverter simpler and more compact, and make its performance faster and more robust. This discussion indicates that the computation burden of the inducverters is much lower than the common synchronization approaches and it has better reliability.

V. COMPARISON WITH SYNCHRONOUS CURRENT CONVERTERS

Using current components for the grid synchronization, synchronous current converters are current-based PLLs as opposed to the conventional voltage-based PLLs [12], [40]. Fig. 5 shows the basic synchronous current converter structure. The synchronous current converters in their initial visions do not have any need for grid voltage information and also voltage sensors after the initial synchronization as grid synchronization and control objectives can be realized using only current information. Therefore, similar to the inducverter in its initial vision, the PLL and voltage sensors can be eliminated after the initial grid synchronization. However, as opposed to the inducverters, synchronous current converters cannot guarantee initial smooth grid connection without an auxiliary synchronization process and unit. Also, any disturbance or deviation in the frequency and angle of grid voltage results in a permanent offset in the output powers as synchronous converters are supposed to inject preset current components/powers at a given frequency which is a critical drawback.

An interesting point of synchronous current converters is that they are single-loop voltage controlled controllers with current control, limitation and regulation capability. In the inducverter, in its initial vision, it is possible to eliminate voltage sensors by using output voltage commands to calculate power as shown in Fig. 4. However, it is also possible to measure three- filter voltages by voltage sensors to control and regulate injected powers to the grid after the filter.

In normal conditions and after initial synchronization, synchronous converters are simpler controllers with lower computation burden as compared with inducverters since they do not have the auxiliary current damping/synchronization unit. Both inducverters and synchronous converters introduce some virtual inertia to power system and can participate in power system frequency control and regulation. Table II shows the comparison between the synchronous converters and inducverters.

TABLE II. COMPARISON OF SYNCHRONOUS CURRENT CONVERTERS AND INDUCVERTERS

Feature	Synchronous current converter	Inducverter
PLL-less grid auto-start		✓
PLL-less operation after initial synchronization	✓	✓
Integrated current-based-PLL and controller	✓	
Voltage-sensor-less operation capability	✓	✓
Constant power generation after disturbance in grid		✓
Single-loop controller	✓	✓
Current control and limitation	✓	✓
Simplicity and very low computation in normal condition	✓	
Virtual inertia for frequency regulation	✓	✓

TABLE III. SIMULATED SYSTEM PARAMETERS

Parameter	Value (SI)
Line inductance	4 mH
Line resistance	0.3Ω
Grid L-L voltage rms	190 v
Filter inductance	1.4 mH
Filter resistance	0.2Ω
DC link voltage	300 v
Virtual rotor momentum (J)	0.1
Virtual damping (D)	4.1
τ_r	0.5
k_1	0.66
k_p	0.005
k_i	0.1
Switching frequency	10 kHz

VI. SIMULATION RESULTS

Performance of the proposed controller is investigated to validate its efficacy in a wide range of operating conditions by simulations carried out in the SIMULINK environment. The simulated system involves one VSC connected to the utility through the filter and line impedances. The controller parameters are given in Table III. To obtain the transfer function of the adaptive virtual impedance, it is necessary to have L_{lr}, R_r, L_{ls}, R_s and L_m. Toward this, the connecting filter can be considered as the virtual stator of the inducverter, so $R_s = 0.3\,\Omega$ and $L_{ls} = 1.4\,mH$. The parameters of the virtual rotor are obtained using τ_r and an equivalent induction machine with $L_{lr} = 2\,mH$ and $L_m = 40\,mH$, so $Z_v = (0.0128 \cdot slip \cdot s + 0.003)/(0.042 \cdot slip \cdot s + 0.01)$. Several scenarios are taken into account presented in the following.

A. *Start-up: soft-synchronization capability and disturbance in the grid frequency*

In this case, the VSC is suddenly connected to the grid at t=0 while no synchronization process and unit are used and the grid information is also not available. It is assumed that grid has rated frequency (60Hz) and voltage amplitude. The real and reactive power references are set to 10 kW and 4kVAr at the moment of grid connection. The power, frequency and current waveforms are shown in Fig. 6. A very smooth grid connection is achieved and the power and frequency reach their steady state conditions within 0.2 s. The initial frequency of the inducverter was set to $\omega_0 = 58.5$ Hz which corresponds to the initial frequency of an induction machine rotor. The power damping unit provides the self-synchronization capability by using output power information and the core power control loops helps the power damping unit to limit and regulate current during grid synchronization to smooth the synchronization and realize soft-start. In the conventional synchronization processes the power references are set to zero during the start-up to prevent huge currents flow to circuit and after synchronization completed the power references are changed to their preset values [10] whereas in this strategy the controller can easily track preset power values even immediately after the start-up period. The proposed method also benefits from a simpler and more compact structure compared to the conventional method and offers a more robust performance as it does not require a dedicated synchronization unit which also in turn eliminates instabilities due to interactions between the converter and the synchronization unit.

At t=0.75 s, the real power reference changes to 8 kW. It is observed that the controller can track reference variations within 0.2 s. At t=2.5 s the grid frequency is reduced by 0.5 Hz. The shown waveforms prove that the inducverter can rapidly adapt itself to the grid frequency variations while the power waveforms are settled in less than 0.1 s. In spite of controllers mimicking synchronous machines like VSGs [15-19], synchronverter [10] and synchronous converters [12], [22-23] the proposed controller can adapt itself with the grid voltage variations without any permanent deviations in the output powers. Actually, in this case the virtual rotor frequency and slip frequency are tuned adaptively by the controller such that the overall frequency becomes equal to the grid frequency and the output power remains constant.

B. *Fault-ride-through capability: disturbance in the grid voltage amplitude and angle jump*

Another salient feature of the self-synchronization of the induction machine is its ability to damp and track grid voltage and angle variations without any information from the grid. To investigate this point, it is assumed that the VSC generates 8kW at 60 Hz and at t=2 s the grid faces an angle jump equal to 15° and at t=3 s the grid voltage is suddenly dropped by 20%. The waveforms of power, frequency and current are presented in Fig. 7. For the case of angle disturbance, after some minor oscillations in the output power and frequency, the controller easily damps power oscillations disturbance within 0.15 s while the frequency settles within 0.5 s. No permanent offset in the output powers occurs. The controller is also capable to easily handle the grid voltage amplitude drop; however, when the angle jump happens, the output currents are slightly increased which is acceptable as VSCs are supposed to tolerate over current for some cycles.

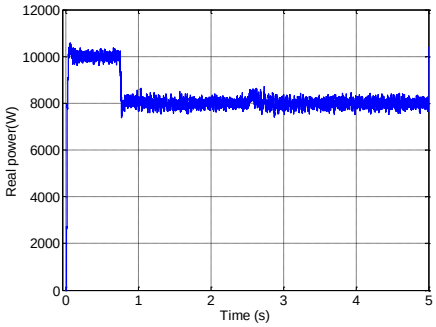

(a)

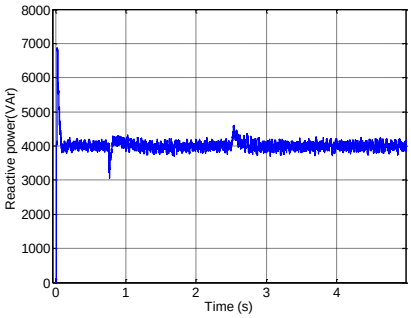

(b)

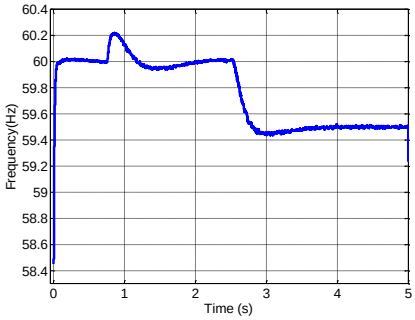

(c)

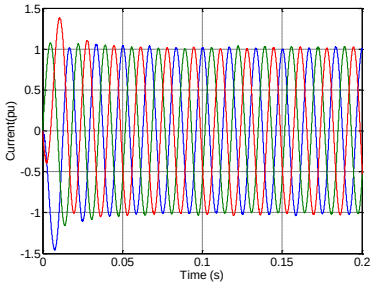

(d)

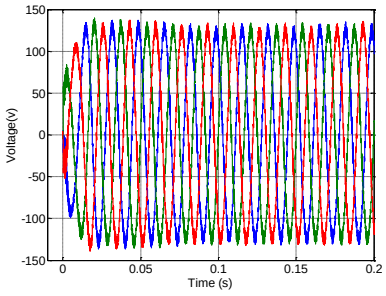

(e)

Fig. 6. Simulation results for case A: (a) real power, (b) reactive power, (c) frequency, (d) instantaneous currents during the start-up, and (e) converter output voltages.

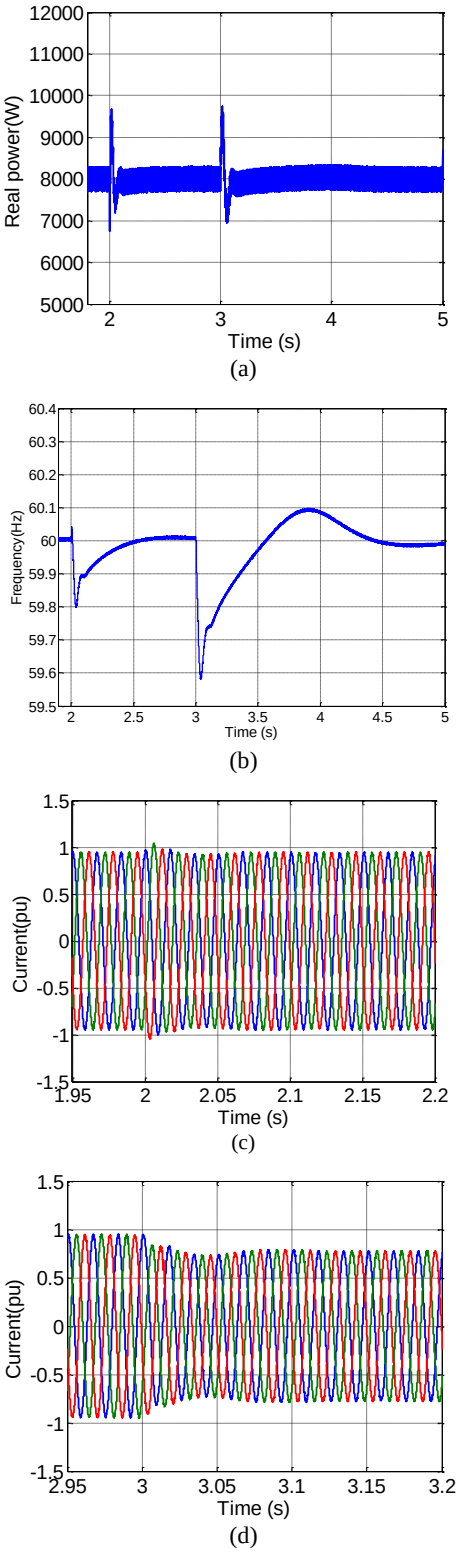

Fig. 7. Simulation results for case B: disturbance in the grid voltage amplitude and angle, (a) real power, (b) frequency, (c) currents subsequent to the angle disturbance, and (d) currents subsequent to the voltage amplitude disturbance.

C. Soft start when grid frequency and voltage amplitude are higher than the rated and disturbance in the DC link voltage

In this case, it is assumed that the VSC is disconnected from the grid and the protection system stops its operation in the islanded mode. Again the breaker is suddenly closed and the grid is restored without any prior synchronization process. In this case,

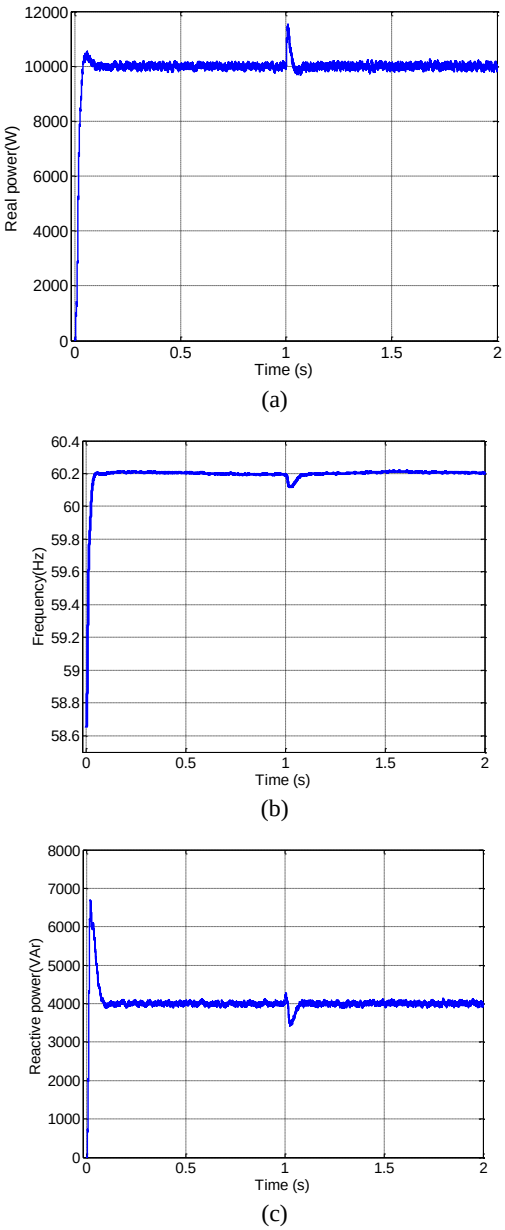

Fig. 8. Simulation results for case C, (a) real power, (b) frequency, and (c) reactive power.

the grid frequency is higher than the rated and is equal to 60.2 Hz and voltage amplitude is 10% higher than the nominal. This is to show effectiveness of the inducverter for soft-start with a grid with frequency and voltage amplitude different from the rated values. The results are shown in. Fig. 8. Although, the grid voltage parameters are different from their rated values, the power damping/soft synchronization unit enables the VSC to synchronize itself with the grid smoothly without considerable overshoot and oscillations while it generates the preset real and reactive powers subsequent to the grid connection. It is seen that variations of the utility voltage parameters do not have effect on the controller performance and the amount of the output power.

Photovoltaic (PV) generation units as the most common form of EI generation units are subject to frequent variation of the output dc-link voltage. Until the dc–link voltage is higher than a specific level the VSC can continue its operation. Also, in the future smart power systems, it is essential that VSCs continue their operation when voltage sag occurs in the grid. To study

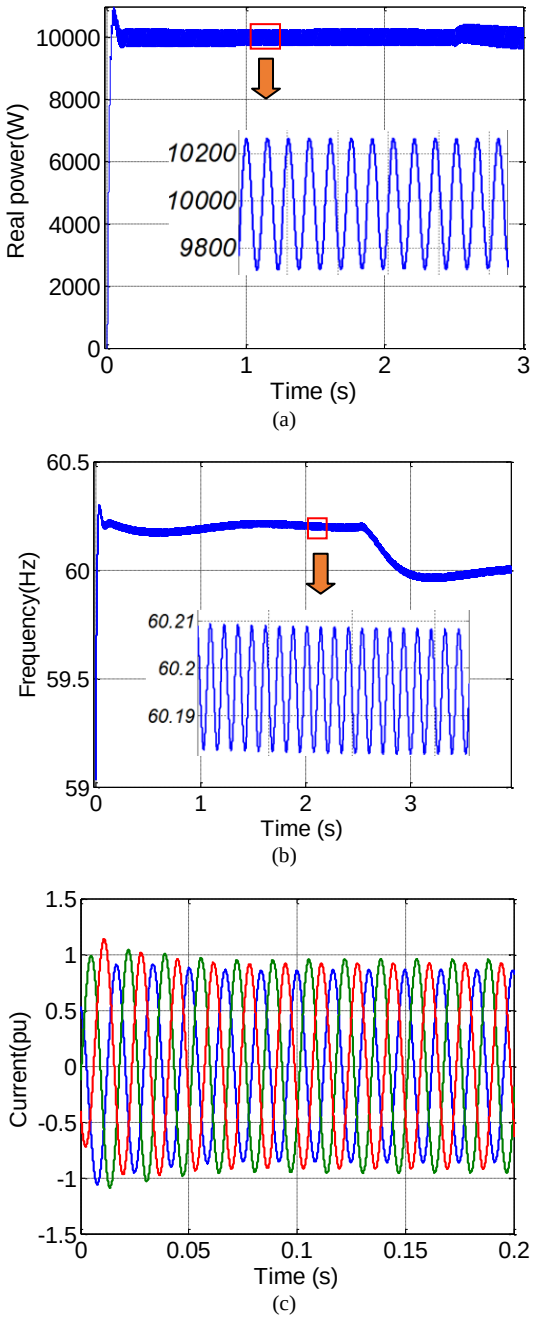

Fig. 9. Inducverter performance under unbalanced line condition: (a) real power, (b) frequency and (c) phase currents (pu).

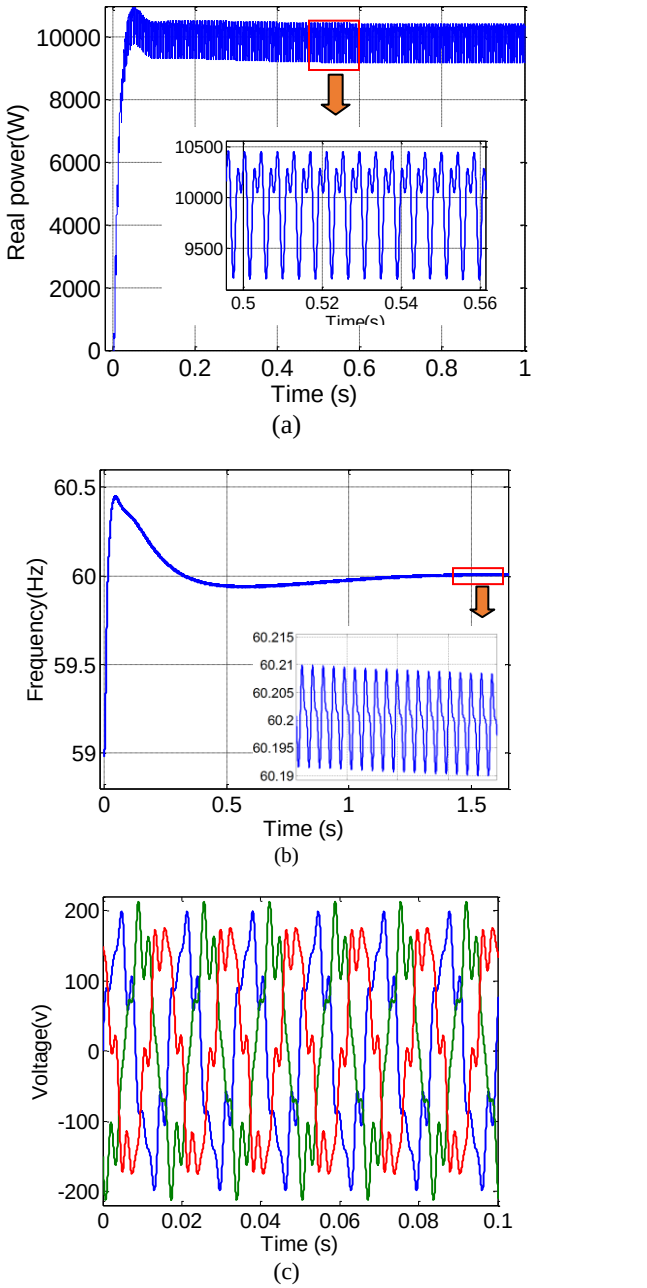

Fig. 10. Inducverter performance under distorted grid condition: (a) real power, (b) frequency and (c) grid voltage.

controller performance in this contingency, the dc-link voltage is changed from 300 v to 350 v at t=1 s. Since the dc-link voltage remains within the thresholds, as shown in Fig. 8, the VSC still can feed the preset powers with appropriate voltage generation. The effect of the dc-link voltage disturbance is almost negligible as controller can easily damp it within 0.15 s by proper adjustment of modulation index. The system is robust against both dc–link and grid voltage variations.

D. Grid synchronization under unbalanced and distorted grid condition

It is important for a VSC to synchronize itself in a polluted grid environment and under unbalanced and/or grid voltage distorted conditions. It is well-known in the literature that induction machines can easily operate under unbalanced conditions. Thus, it is expected that inducverters present smooth and stable operation and synchronization in polluted grids. This is because of two main reasons: first using virtual torque/power as the feedback signal for synchronization has better performance since voltage oscillations are less pronounced in the output power, power-based inducverter has better performance than conventional voltage-based PLLs. Second, the virtual inertia term in the synchronization unit act like a low-pass filter, so it filters out ripples and fluctuations due to voltage distortions and as a result frequency is not almost affected. Despite, voltage-based PLLs are sensitive to voltage distortions and need some techniques to overcome this difficulty.

Toward this, two scenarios are considered shown in Figs. 9 and 10. In the first, the VSC is connected to a grid with frequency of 60.2 Hz through unbalanced lines and grid frequency reduces to

TABLE IV
PARAMETERS OF THE SYNCHRONOUS CURRENT CONVERTER

Parameter	Value (SI)
k_p	10
k_f	12
k_d	0.8
k_q	0.5
k_{qi}	50
DC link voltage	450

60 Hz at t=2.5 s. The line impedances are $Z_a = 0.4 + j1.885\ \Omega$, $Z_b = 0.3 + j1.508\ \Omega$ and $Z_c = 0.35 + j1.696\ \Omega$ showing more than 25% impedance mismatch between the connecting lines. Fig. 9 shows the corresponding waveforms. To show power oscillations in a better way and eliminate switching effects, average model of VSC is used in this case. Ripples with amplitude of 550 W appear in the output real power. The frequency ripple in the steady state is limited to 0.024 Hz due filtering effect of the virtual rotor. At t=2.5 s, the grid frequency returns to its rated value, i.e. 60 Hz and as shown in Fig. 9, the VSC can easily track grid voltage frequency variation.

In the second scenario, the grid voltage has fifth and seventh order harmonics equal to 20% and 15% of the fundamental harmonic, respectively. Fig. 10 shows the corresponding results for this case. The currents are totally distorted, however, the connection is still successful and power and frequency waveforms show ripples less than 1100 W and 0.029 Hz, respectively. Actually, the effects of current and power harmonics are almost filtered-out in the synchronization unit because of the virtual rotor resulting in stable synchronization and performance.

E. Comparison with synchronous current converters

As mentioned earlier, inducverters offer some advantages over synchronous converters. To investigate these superiorities, some simulations are carried out using the controller shown in Fig. 5. The controller parameters are given in Table IV and are tuned such that the fastest response with steady state error less than 0.5% are achieved. d- and q-axis current references are set such that in the steady state converter generates P=10000 W and Q=4000 VAr. In the first case, a synchronization process is used to match frequency, angle and amplitude of voltages of both sides of the switch at the moment of connection to provide smooth grid synchronization. At t=1 s, the grid frequency reduces to 59.5 Hz, and at t=2 s the grid frequency returns to its rated value, i.e. 60 Hz. As it can be seen from Fig. 11, although subsequent to the grid connection overall system operation is good, the output powers are oscillatory for some cycles, some minor overshoot is observed, and the settling time is 0.5 s which is larger than the settling time of the inducverter (less than 0.1 s). When disturbance in the grid frequency occurs, the synchronous current converter can easily tracks its variations using only local current information without any voltage sensor or PLL. However, a major drawback related to synchronous current converters can be seen from Fig. 11 that a grid frequency variation at t =1 s results in a permanent offset in the output powers where real power increases to about 16 kW. In the second case, shown in Fig. 12, it is assumed that at the moment of connection there is an angle

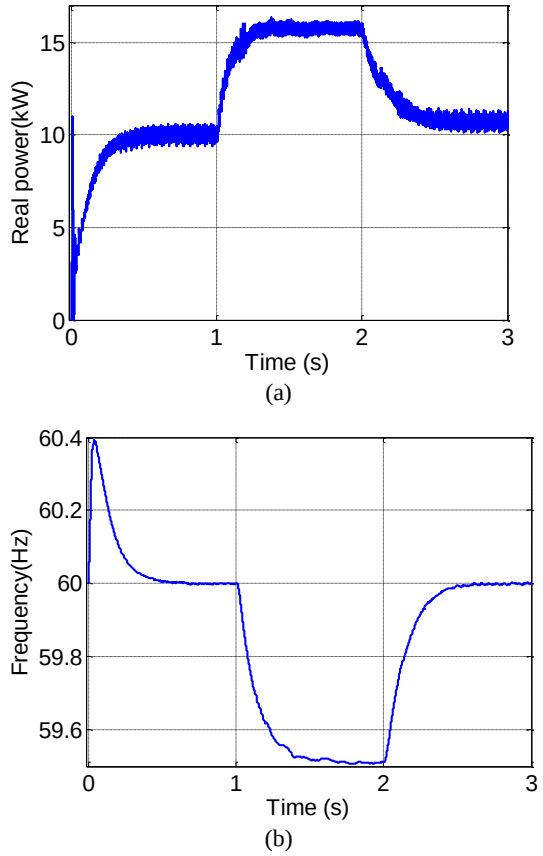

Fig. 11. Performance of synchronous current converter subsequent to grid connection using the standard synchronization process, (a) real power and (b) frequency.

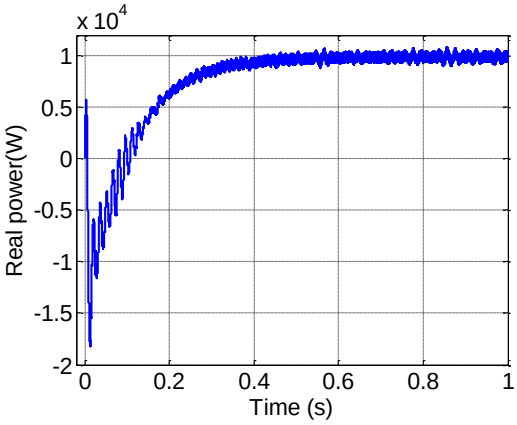

Fig. 12. Real power waveform of synchronous current converter in the case of 30° out-of-phase breaker closing.

mismatch of 30° between two sides of the breaker. Subsequent to the grid connection, the output real power may be increased to about twice of the steady state values which may cause protection system act. However, the synchronous current converter is still able to synchronize itself with the grid and reach its steady state value within 0.8 s.

VII. REAL-TIME-HIL RESULTS

The effectiveness of the proposed inducverter is validated in a dSPACE 1006 based real-time HIL system. A VSC is connected to an ideal utility grid through a breaker, an RL filter and a connecting line.

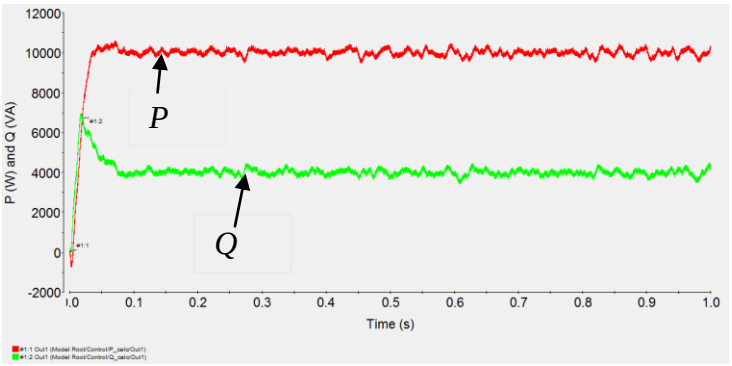

(a)

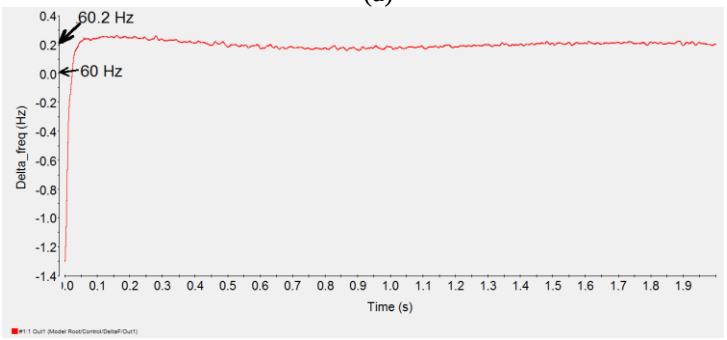

(b)

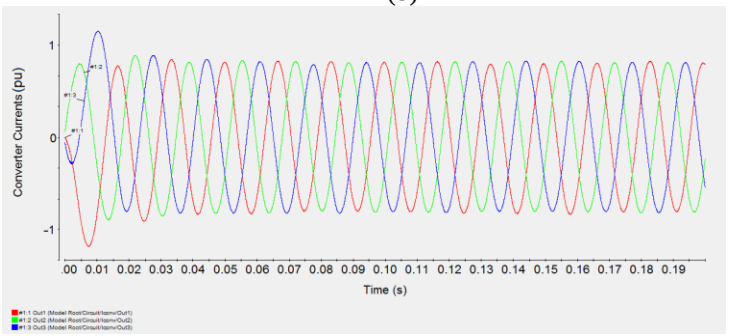

(c)

Fig. 13. Real-time HIL results for auto-synchronization with a grid with frequency of 60.2 Hz, (a) real and reactive powers, (b) frequency deviation (Hz), and (c) output currents (pu).

The breaker is located at the PCC. The HIL model implements a multirrating emulation of the circuit:

a) The power circuit, which includes a programmed voltage source with 61.2 Hz as the grid frequency at the moment of connection and the power converter, has been implemented in a piece of code running at 2.5e-5 s.

b) The control algorithm works at a sampling rate of 2e-4s, and sets the reference of the power converter.

This set-up permits to test the suiability of the discrete-time control algorithm working in a frequency-deviated environment, which is not feasible to reproduct with real hardware. Two different scenarios are taken into account as follows:

A. Auto-start with a grid with frequency of 60.2 Hz

In this case, to show the ability of the inducverter to automatically synchronize itself with a grid with unknown frequency, it is assumed the grid is initially working at frequency of 60.2 Hz which is different from its rated value, i.e. 60 Hz, and voltage amplitude is also 5% higher than its rated value. The switching frequency is 5 kHz. No PLL or synchronization

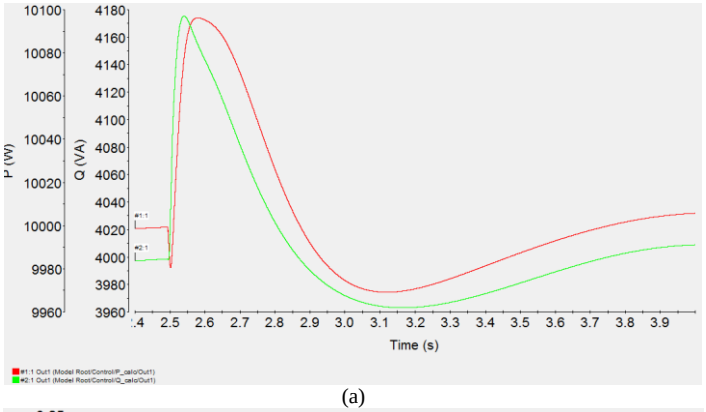

(a)

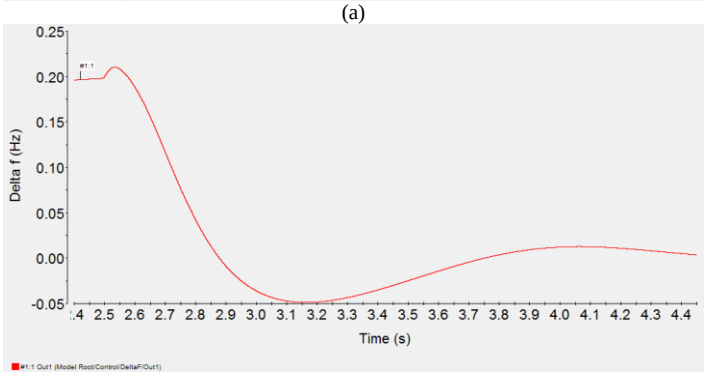

(b)

Fig. 14. Real-time HIL results for variation in grid frequency, (a) average real and reactive powers and (b) frequency deviation from 60 Hz.

process is used. The breaker is suddenly closed and this moment is considered as the reference of time, i.e. t=0. The corresponding power, current and frequency deviation waveforms are shown in Fig. 13. Although the grid frequency is 60.2 Hz, the inducverter can easily synchronize itself with the grid using local current information. Actually, the controller generates some synchronizing and damping current by proper angle adjustment providing smooth grid auto-synchronization. It should be noted that for better resolution frequency deviation from 60 Hz is shown and the initial frequency is set to 58.7 Hz. The settling times for real and reactive powers are less than 0.1 s.

B. Disturbance in the grid frequency

In the second scenario, at t=2.5 s the grid frequency returns from 60.2 Hz to its rated value, i.e. 60 Hz. The corresponding waveforms of average real and reactive powers and frequency are shown in Fig. 14. Again, the inducverter is able to track variations of grid frequency using current information. It is also seen that after some minor oscillations, the inducverter inject constant amount of power to grid regardless of grid frequency.

VIII. Experimental Results

The start-up operation has been performed in a lab scale. A 2.2 kW Danfoss power converter driven by dSpace 1006 is employed for that purpose. The grid voltage is 230 Vrms. The active power and reactive power references have been set to 1500 W and 750 VA, respectively. Fig. 15 (a) shows the active power and reactive power during the start up. Fig. 15 (b) shows the current during the start up. These results obtained at a lab-scale prototype match the time responses predicted by the simulation models. Please note that an RL filter instead of LC filter is used which results in high noise in the output powers due to switching effect.

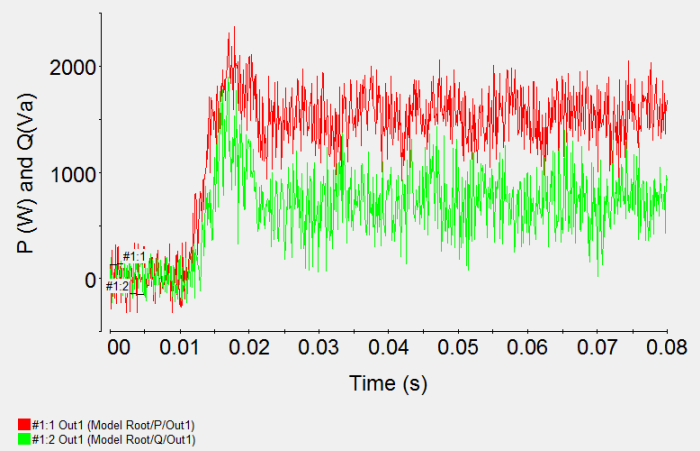

(a)

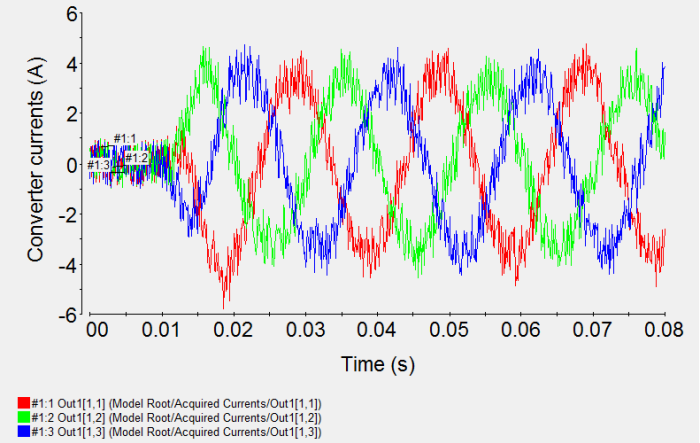

(b)

Fig. 15. Experimental results for an inducverter with RL filter, (a) real and reactive powers and (b) three-phase currents.

IX. Conclusions

A new control strategy was developed for the integration of VSCs to smart grids with soft-start and virtual inertia capability. The controller has two main parts. The current damping/synchronization unit provides self-synchronization and self-start capability for VSCs for by using output current information without any information from the grid. The focus of this paper is to substitute synchronization and PLL algorithms by control blocks which emulate the induction machine dynamics. Then, the proposed inducverter has the following features: it has self-start and is adaptive to the grid voltage frequency and amplitude variations. The proposed controller can significantly reduce computation burden and improve system stability by elimination of PLL. The proposed controller also introduces some emulated inertia to power system helping frequency regulation in the future smart power systems with overall low inertia of VSCs. The paper extends the previous works in [1], [12], [22-23], [40] to form a unified set of controllers for the smart grid integration.

References

[1] M. Ashabani and Y. A. R. –I. Mohamed, "Novel comprehensive control framework for incorporating VSCs to smart power grids using bidirectional synchronous-VSC," *IEEE Trans. Power Syst.*, vol. 29, no. 2, pp. 943-957, 2014.

[2] ECPE European Center for Power Electronics, "Strategic research agenda on intelligent power electronics for energy efficiency," Jan. 2008.

[3] A. K. Srivastava, A.A. Kumar, and N.N. Schulz, "Impact of distributed generations with energy storage devices on the electric grid," *IEEE Syst. J.*, vol. 6, no. 1, p. 100-117, Mar. 2012.

[4] S. Eftekharnejad, V. Vittal, G. T. Heydt, B. Keel, and J. Loehr, "Impact of increased penetration of photovoltaic generation in power systems," *IEEE Trans. Power Syst*, vol. 28, no. 2, 893-901, 2013.

[5] A. Azmy and I. Erlich, "Impact of ddistributed generation on the stability of electrical power system," in *Proc. IEEE Power Eng. Soc. Gen. Meeting*, 2005, pp. 1056-1063.

[6] A. H. K. Alanoudy, H.H. Zeineldin, and J. L. Kirtley, "Microgrid stability characterization subsequent to fault triggered islanding incidents," *IEEE Trans. Power Del*., vol. 27, no. 2, pp. 658-669, Apr. 2012.

[7] J. G. Slootweg and W. L. Kling, "Impact of distributed generation on power system transient stability," in *Proc. IEEE Power Eng. Soc. Summer Meeting*, 2002, pp. 863-867.

[8] Z. Ye *et al*, "Study and development of anti-islanding control for grid-connected inverter," NREL/SR-560-36243, 2004.

[9] L. Zhang, L. Harnefors, and H. -P. Nee, "Power-synchronization control of grid-connected voltage-source converters," *IEEE Trans. Power Syst.*, vol. 25, no. 2, pp. 809–819, May 2010.

[10] Q. –C. Zhong, P. –L. Nguyen, Z. Ma, W. Sheng, "Self-synchronized synchronverters: inverters without a dedicated synchronization unit," *IEEE Trans. Power Elctron*., vol. 29, no. 2, pp. 617-630, 2014.

[11] H. Alatrash, A. Mensah, E. Mark, G. Haddad, and J. Enslin, "Generator emulation controls for photovoltaic inverters," *IEEE Trans. on Smart Grid*, vol.3, no.2, pp.996-1011, June 2012.

[12] M. Ashabani and Y. A. -R. I. Mohamed, "New family of microgrid control and management strategies in smart distribution grids-analysis, comparison and testing," *IEEE Trans. Power Syst*., vol. 29, no. 5, pp. 2257-2269, Sep., 2014.

[13] J. Zhu, C. D. Booth, G. P. Adam, A. J. Roscoe, and C. G. Bright, "Inertia emulation control strategy for VSC-HVDC transmission systems," *IEEE Trans. Power Syst*., vol 28, no. 2, pp. 1277-1287, 2013.

[14] A.A.A. Radwan and Y. A. –R. I. Mohamed, "Stabilization of Medium-Frequency Modes in Isolated Microgrids Supplying Direct Online Induction Motor Loads," *IEEE Trans. Smart Grid*, vol. 5, no. 1, pp. 358-370, 2014.

[15] J. Driesen and K. Visscher, "Virtual synchronous generators," *IEEE Power and Energy Society General Meeting-Conversion and Delivery of Electrical Energy in the 21st Century*, 2008.

[16] J. Alipour, Y. Miura, and T. Ise, "Distributed generation grid integration using virtual synchronous generator with adoptive virtual inertia," in *Proc. IEEE Energy Conv. Cong. And Exp.*, pp. 4546-4552, 2013.

[17] M. Torres, "Integration of a large-scale photovoltaic plant using a multilevel converter topology and virtual synchronous generator control," in *Proc. 23rd IEEE Int. Symp. On Ind. Electron.* pp. 2620-2624, 2014.

[18] T. Vu Van et al, "Virtual synchronous generator: an element of future grids," 2010 IEEE PES Innovative Smart Grid Technologies Europe, Gothenburg, Oct, 2010.

[19] H. P. Beck and R. Hesse, "Virtual synchronous machine," in *Proc. IEEE EPQU Conf*., pp. 1–6, 2007.

[20] M. Datta, H. Ishikawa, H. Naitoh, and Senjyu, "LFC by coordinated virtual inertia mimicking and PEVs in power utility with MW-class distributed PV generation," in *Proc. IEEE 13rd Workshop Cont. Mod. For Power Electron.*, 2012.

[21] S. D'Arco, J. A. Suul, O. B. Fosso, " Control system tuning and stability analysis of Virtual Synchronous Machines," in *Proc. 2013 IEEE Energy Conv. Cong. and Exp. (ECCE)*, Colorado, USA, 2013.

[22] M. Ashabani and Y. A. -R. I. Mohamed, "Integrating VSCs to weak grids by nonlinear power damping controller with self-synchronization capability," *IEEE Trans. Power Syst*., vol. 29, no. 2, pp. 805-804, 2014.

[23] M. Ashabani and Y. A. –R. I. Mohamed, "General interface for power management of micro-grids using nonlinear cooperative droop control," *IEEE Trans. Power Syst*., vol. 28, no. 3, pp. 2929-2941, Aug. 2013.

[24] J. Meng, X. Shi, Y. Wang, and C. Fu, "A virtual synchronous generator control strategy for distributed generation," 2014 China Int. Conference on Electricity Distribution (CICED), Shengen, China, 2014.

[25] T. L. Vandoorn *et al*, "Directly-coupled synchronous generators with converter behavior in islanded microgrids," *IEEE Trans. Power Syst.*, vol. 27, no. 3, pp.1395-1406, Aug. 2012.

[26] F. Blaabjerg, R. Teodorescu, M. Liserre, and A. V. Timbus, "Overview of control and grid synchronization for distributed power generation systems," *IEEE Trans. Ind. Electr*., vol. 53, no. 5, pp. 1398-1408, Oct. 2006.

[27] Y. Wang and Y. Li, "Grid synchronization PLL based on cascaded delay signal cancellation," *IEEE Trans. Power Electron*., vol. 26, no. 7, 1987-1997, Jul. 2011.

[28] A. H. Norouzi, A. M. Sharaf, "Two control scheme to enhance the dynamic performance of the STATCOM and SSSC," *IEEE Trans. Power Del.*, vol. 20, pp. 435-442, Jan. 2005.

[29] D. Dong, B. Wen, D. Boroyevich, P. Mattavelli, and Y. Xue, "Analysis of phase-locked loop low frequency stability in three-phase grid-connected power converters impedance interactions," *IEEE Trans. Ind. Electron.*, vol. 62, no. 1, pp. 310-321, 2015.
[30] G. Escobar et al, "Fixed-reference-frame phase-locked-loop with fast line-voltage amplitude tracking," *IEEE Trans. Ind. Electron*, vol. 58, no. 5, pp. 1943-1951, May 2011.
[31] C. Da Silva *et al*, "A digital PLL scheme for three-phase system using modified synchronous reference frame," *IEEE Trans. Ind. Electron*, vol. 57, no.11, pp. 3814-3821, Nov. 2010.
[32] K. J. Lee, "A novel grid synchronization PLL method based on adaptive low-pass filter for grid-connected PCS," *IEEE Trans. Ind. Electron.*, vol. 61, pp. 292-301, 2014.
[33] S. M. Ashabani and Y. A. -R. I. Mohamed, "A flexible control strategy for grid-connected and islanded microgrids with enhanced stability using nonlinear microgrid stabilizer," *IEEE Trans. Smart Grid*, vol. 3, no. 3, pp. 1291-1301, Sep. 2012.
[34] R. W. De Doncker and D. W. Novotny, "The universal field oriented control," *IEEE Trans. Ind. Appli*., vol. 30, pp. 92-100, Jan./Feb., 1994.
[35] J. L Kirtley, 'Introduction to power systems' chapter 10, MIT open course ware, 2003.
[36] S. Golestan, F.D. Freijedo, J. M. Guerrero, "A systematic approach to design high-order phase-locked loops," *IEEE Trans. Power Electron.*, vol. 30, no. 6, pp. 2885-2890, 2015.
[37] S. Golestan, F.D. Freijedo, A. Vidal, J. M. Guerrero, "A quasi-type-1 phase-locked loop structure," *IEEE Trans. Power Electron*., vol. 29, no. 12, pp. 6264-6270, 2014.
[38] "IEEE guide for design, operation, and integration of distributed resource island systems with electric power Systems," *IEEE Std 1547.4-2011*, pp.1-54, July 20 2011.
[39] J. C. Vasquez, J. M. Guerrero, Jaume Miret, and L. G. D. Vicuna, "Hierarchical control of intelligent microgrids," *IEEE Ind. Electron. Mag*., pp. 23- 29, Dec. 2010.
[40] M. Ashabani, Y. Mohamed, M. Mirsalim, and M.Aghashabani, "Multivariable droop control of synchronous current converters in weak grids/microgrids with decoupled dq-axes currents," *IEEE Trans. Smart Grid*, vol. 6, pp.1610-1620, no. 4, July 2015.
[41] P. Anderson and A. A. Fouad, Power System Stability and Control, Ames, IA, Iowa State University, Press 1977.

Mahdi Ashabani received the B.S. degree in electrical engineering from the Isfahan University of Technology, Isfahan, Iran; the M.Sc. degree in power engineering from the Amirkabir University of Technology (Tehran Polytechnic), Tehran, Iran, in 2009; and the Ph.D. degree in power engineering and power electronics from the University of Alberta, Edmonton, AB, Canada, in 2014.
He is currently with American University in Dubai as an assistant professor. His current research interests include operation of smart grids, control of voltage source converters in powers systems, design and optimization of electric machines, renewable energy, and hybrid vehicles.

{Francisco D. Freijedo} (M'07) received the M.Sc. degree in Physics from the University of Santiago de Compostela, Santiago de Compostela, Spain, in 2002 and the Ph.D. degree from the University of Vigo, Vigo, Spain, in 2009.
From 2005 to 2011, he was a Lecturer with the Department of Electronics Technology of the University of Vigo. From 2011 to 2014, he worked in the wind power industry as a control engineer.
Since 2014, he is a Postdoctoral Researcher at the Department of Energy Technology of Aalborg University. His main research interests are in the areas of ac power conversion.

Saeed Golestan (M'11-SM'15) received the B.Sc. degree in electrical engineering from Shahid Chamran University of Ahvaz, Ahvaz, Iran, in 2006, and the M.Sc. degree in electrical engineering from the Amirkabir University of Technology, Tehran, Iran, in 2009. He is currently with the Department of Energy Technology, Tehran, Iran, in 2009. He is currently with the Department of Energy Technology of Aalborg University, Denmark. From 2009 to 2015, he was a Lecturer in the Department of Electrical Engineering, Abadan Branch, Islamic Azad University, Tehran, Iran. His research interests include phase-locked loop and nonlinear filtering techniques for power and energy applications, power quality measurement and improvement, estimation of power systems, and microgrid.

{Josep M. Guerrero} (S'01-M'04-SM'08-FM'15) received the B.S. degree in telecommunications engineering, the M.S. degree in electronics engineering, and the Ph.D. degree in power electronics from the Technical University of Catalonia, Barcelona, in 1997, 2000 and 2003, respectively. Since 2011, he has been a Full Professor with the Department of Energy Technology, Aalborg University, Denmark, where he is responsible for the Microgrid Research Program. From 2012 he is a guest Professor at the Chinese Academy of Science and the Nanjing University of Aeronautics and Astronautics; and from 2014 he is chair Professor in Shandong University.
His research interests is oriented to different microgrid aspects, including power electronics, distributed energy-storage systems, hierarchical and cooperative control, energy management systems, and optimization of microgrids and islanded minigrids. In 2014 he was awarded by Thomson Reuters as ISI Highly Cited Researcher, and in 2015 same year he was elevated as IEEE Fellow for contributions to "distributed power systems and microgrids."